TRB

TRANSPORTATION RESEARCH RECORD

Journal of the Transportation Research Board, No. 2259

Traffic Signal Systems 2011

TRANSPORTATION RESEARCH BOARD
OF THE NATIONAL ACADEMIES

Quantifying Dynamic Factors Contributing to Dilemma Zone at High-Speed Signalized Intersections

Heng Wei, Zhixia Li, Ping Yi, and Kevin R. Duemmel

The issue of the dynamic yellow light dilemma zone (DZ) has been raised by researchers for many years. However, quantitative study of the inherent factors contributing to the dynamic DZ remains an issue, perhaps because of the lack of effective means for collecting the trajectory data. This paper presents an analysis of the dynamic characteristics of major contributing factors for Type I DZ and the option zone on the basis of vehicle trajectory data during yellow intervals. The qualified trajectory data of 1,445 vehicles were extracted from 46-h high-resolution videos shot at four high-speed signalized intersections in Ohio with the use of the cost-effective software VEVID, developed and upgraded by the first two authors. The statistical analysis of the obtained trajectory data quantitatively revealed the dynamic nature of major DZ contributing factors. Results indicated that the minimum perception–reaction time of drivers was greatly influenced by speed and could be modeled as a function of the speed. The maximum deceleration rate for stopping and the maximum acceleration rate for running a yellow light were greatly dependent on speed and the 85th percentile speed of the intersection approach. The rates could be expressed as a function of those two variables. On the basis of the new findings, the traditional Type I DZ model was greatly modified and improved. The new model provides a theoretical base for updating the existing DZ tables with the identified dynamic characteristics of the contributing factors.

At high-speed signalized intersections (i.e., posted speed limit is 40 mph or higher), the yellow light dilemma is widely known as a major cause of rear-end and right-angle crashes. The so-called dilemma literally reflects the drivers' indecisiveness when making stop or go decisions in response to yellow indications. However in practice, the dilemma can be physically characterized by a zone in advance of the intersection, which is known as the dilemma zone (DZ). Vehicles in the DZ at the onset of the yellow indication cannot either clear the intersection during the yellow interval or safely stop before the stop line. This concept was initially proposed by Gazis et al. (*1*) and is known by researchers as the Type I DZ (*2–6*).

H. Wei, 792 Rhodes Hall, P.O. Box 210071, and Z. Li, 735 Engineering Research Center, School of Advanced Structures, Advanced Research in Transportation Engineering Systems Laboratory, College of Engineering and Applied Science, University of Cincinnati, Cincinnati, OH 45221. P. Yi, Department of Civil Engineering, Ohio Transportation Consortium, University of Akron, Akron, OH 44325. K. R. Duemmel, Ohio Department of Transportation, Office of Traffic Engineering, 1980 West Broad Street, Columbus, OH 43223. Corresponding author: H. Wei, heng.wei@uc.edu.

Transportation Research Record: Journal of the Transportation Research Board, No. 2259, Transportation Research Board of the National Academies, Washington, D.C., 2011, pp. 202–212.
DOI: 10.3141/2259-19

Another definition of DZ, which was proposed by Zegeer in 1977, is "the roadway segment where more than 10% and less than 90% of the drivers would choose to stop." (*7*). This definition has been further named the Type II DZ or the indecision zone (*8–14*).

Urbanik and Koonce conducted a comprehensive literature review to clarify the confusion between the two types of DZs (*15*). They concluded that the Type I DZ could be eliminated by a prolonged yellow interval, whereas the Type II DZ can be minimized only by applying the detection-based DZ protection systems (*12–14*). However, previous studies have also proved that a longer yellow interval could eliminate only the Type I DZ, but would produce a longer option zone (*16, 17*), which is still a safety concern. The option zone is closely related to the Type I DZ. It is defined as the zone in which vehicles at the onset of the yellow indication can either clear the intersection during the yellow time or safely stop before the stop line. Drivers in the option zone will also experience indecisiveness (dilemma) when making stop and go decisions, which makes them still highly exposed to rear-end or right-angle crashes.

The mathematical model representing the Type I DZ and the option zone is called the Gazis, Herman, and Maradudin (GHM) model (*18*). According to the GHM model, the location of the Type I DZ and the option zone is determined by the minimum stopping distance (X_c) and the maximum yellow light running distance (X_0), given a particular length of yellow interval. When X_c is greater than X_0, the Type I DZ forms. When X_0 is greater than X_c, the option zone exists. X_0 and X_c can be computed by using the following contributing factors: speed of vehicle (V_0), minimum perception–reaction time (PRT) for stopping ($\hat{\delta}_{Stop}$), maximum deceleration rate for stopping ($\hat{a}_{Stop}$), minimum PRT for running ($\hat{\delta}_{Run}$), maximum acceleration rate ($\hat{a}_{Run}$) for running, duration of yellow interval (τ), intersection width (W), and vehicle length (L).

In most engineering practice, the contributing factors such as $\hat{a}_{Stop}$, $\hat{a}_{Run}$, and $\hat{\delta}_{Stop}$ are assumed to have constant values. For example, in ITE's *Traffic Engineering Handbook*, $\hat{a}_{Stop}$, $\hat{a}_{Run}$, and $\hat{\delta}_{Stop}$ are assumed to be constants, 10 ft/s^2, 0 ft/s^2, and 1 s, respectively (*19*). FHWA suggests in the *Traffic Detector Handbook* that $\hat{a}_{Stop}$ could alternatively be a constant value of 16 ft/s^2 in some cases (*20*). AASHTO suggests 11.2 ft/s^2, 0 ft/s^2, and 1.5s for $\hat{a}_{Stop}$, $\hat{a}_{Run}$, and $\hat{\delta}_{Stop}$, respectively (*21*). At most times, $\hat{a}_{Run}$ is assumed to be 0 ft/s^2. However, in the GHM model, $\hat{a}_{Run}$ was originally considered as a linear function of speed with a negative slope (*1*); this function is also reflected in FHWA's *Traffic Detector Handbook* (*20*).

The research of Liu et al. started to consider nonconstant contributing factors for the Type I DZ and option zone (*3*). In their study, they classified drivers into three categories and used different values of contributing factors for different categories of drivers when the DZs were computed.

The previous studies conducted by the authors have raised the discussion that values of the contributing factors of Type I DZ (i.e., $\hat{a}_{Stop}$, $\hat{a}_{Run}$, $\hat{\delta}_{Stop}$ and $\hat{\delta}_{Run}$) might be dynamic with different approach speeds, and the results have also proved that dynamic (*22*, *23*). However, whether these contributing factors are related only to speed or are also dynamic with other potential variables, such as the duration of the yellow time and the 85th percentile speed of the intersection approach, still needs to be further investigated. Therefore, this paper is dedicated to analyzing the dynamic characteristics of the major contributing factors for Type I DZ and option zone and their correlation with speed, duration of yellow time, and 85th percentile speed of the intersection approach.

DYNAMIC DZ MODEL

Under the assumption that $\hat{a}_{Stop}$, $\hat{a}_{Run}$, $\hat{\delta}_{Stop}$, and $\hat{\delta}_{Run}$ are functions of speed (V_0), duration of yellow time (τ) and 85th percentile speed (V_{85th}), the following dynamic DZ model, which modifies the original GHM model by changing the constant factor values into dynamic ones, is tentatively proposed.

$$X_c(V_0, \tau, V_{85th}) = V_0\hat{\delta}_{stop}(V_0, \tau, V_{85th}) + \frac{V_0^2}{2 \cdot \hat{a}_{stop}(V_0, \tau, V_{85th})} \quad (1)$$

$$X_0(V_0, \tau, V_{85th}) = V_0\tau + \frac{1}{2}\hat{a}_{Run}(V_0, \tau, V_{85th}) \cdot \left[\tau - \hat{\delta}_{Run}(V_0, \tau, V_{85th})\right]^2 \quad (2)$$

where

V_0 = vehicle's approaching speed (ft/s),
$X_c(V_0, \tau, V_{85th})$ = critical (minimum) stopping distance from stop line at speed V_0 and under yellow interval τ and 85th percentile speed V_{85th} (ft),
$X_0(V_0, \tau, V_{85th})$ = maximum yellow light running distance from stop line at speed V_0 and under yellow interval τ and 85th percentile speed V_{85th} (ft),
$\hat{\delta}_{Stop}(V_0, \tau, V_{85th})$ = minimum PRT for stopping at speed V_0 and under yellow interval τ and 85th percentile speed V_{85th} (s),
$\hat{a}_{Stop}(V_0, \tau, V_{85th})$ = maximum deceleration rate for stopping at speed V_0 and under yellow interval τ and 85th percentile speed V_{85th} (ft/s^2),
$\hat{\delta}_{Run}(V_0, \tau, V_{85th})$ = minimum PRT for yellow light running at speed V_0 and under yellow interval τ and 85th percentile speed V_{85th} (s), and
$\hat{a}_{Run}(V_0, \tau, V_{85th})$ = maximum acceleration rate for yellow light running at speed V_0 and under yellow interval τ and 85th percentile speed V_{85th} (ft/s^2).

In the case in which $X_c > X_0$, the Type I DZ is formed, and the roadway segment between X_c and X_0 is the Type I DZ. However, in the case in which $X_c < X_0$, the Type I DZ is eliminated, and the roadway segment between X_0 and X_c is the option zone.

The selection of parameters (i.e., V_0, τ, V_{85th}) in the models of $\hat{a}_{Stop}$, $\hat{a}_{Run}$, $\hat{\delta}_{Stop}$, and $\hat{\delta}_{Run}$ is temporary. The final models will include only the significant parameters based on the final results from the statistical analyses. Also, the intersection width (W) and vehicle length (L) are removed from the original GHM model. The reason is that on the basis of field observations, when drivers perceive the yellow indication, they do not consider whether they could clear the intersection completely during the yellow interval. Actually, their concern is whether they could pass the stop line before the onset of the red indication.

DATA COLLECTION

Four approaches of high-speed signalized intersections in Ohio are selected as the study sites and are summarized in Table 1. All the study sites are located in suburban areas. No DZ protection is implemented and no advance detectors are installed. At each study site, a high-definition digital video camera was placed on the top of a van parked on the shoulder of the intersection approach to shoot vehicle maneuvers during the yellow intervals. An attempt was made to place the camera far enough to cover all possible yellow light running distances. In total, 46-h video data were collected at the four study sites, covering different periods of the day. The video was then converted to AVI format with a frame rate of 30 frames per second and a resolution of 1,280 pixels × 720 pixels.

The video-capture-based software VEVID was used to obtain time-based trajectory data of vehicles during the yellow intervals (*24*). Vehicles targeted for trajectory data extraction include all yellow light running vehicles, all red light running vehicles, and vehicles that are the first stopped (first-to-stop) vehicles in their lanes during the yellow intervals. Only vehicles that go straight were targeted for data extraction. Although two of the study sites have a shared through and right-turn lane, only those yellow intervals in which no right-turn vehicles

TABLE 1 Conditions of Study Sites and Data Collection

Condition	OH-4 at Boymel	OH-14 at OH-44	OH-4 at Seward	US-50 at OH-128
Posted speed limit	50 mph	50 mph	50 mph	55 mph
85th percentile speed	47.4 mph	51.7 mph	44.5 mph	58.3 mph
Yellow time	4.0 s	4.0 s	4.5 s	5.0 s
Through lanes	2 dedicated	1 dedicated 1 shared	2 dedicated	1 dedicated 1 shared
Distance covered by camera	420 ft	460 ft	420 ft	480 ft
First-to-stop samples	150	92	158	74
Run-yellow samples	253	62	403	178
Run-red samples	25	22	18	10

are involved are targeted for data extraction. The extracted trajectory data include the following items:

- Vehicle's speed at the onset of yellow indication,
- Vehicle's distance from stop line at the onset of yellow indication,
- Time used by a running vehicle to reach the stop line calculated from the onset of yellow, and
- ID of the video frame in which the brake light of a stopped vehicle is illuminated.

The details about how to extract the trajectory data can be found in previous studies (*22, 23*). Finally, trajectory data of 1,445 vehicles (speed ≥ 30 mph) were extracted and collected. Table 1 provides the detailed information about the four study sites and the number of data samples at each study site.

In Table 1, the rows "first-to-stop samples," "run-yellow samples," and "run-red samples" list the total number of observed vehicles that first stopped in their lane during the yellow interval, ran yellow, and ran red, respectively. According to Table 1, the posted speed limit is either 50 mph or 55 mph at the four study sites. However, various 85th percentile speeds were found, ranging from 47.4 mph to 58.3 mph. The yellow time is also various at the four study sites, including 4.0 s, 4.5 s, and 5.0 s. This variety of data provides ideal samples for analyzing the effect of yellow time and 85th percentile speed on the DZ contributing factors.

ANALYSIS OF MINIMUM PRT AND MAXIMUM DECELERATION RATE

Preparation of Data Samples

First, the PRT and the deceleration rate of each sample vehicle need to be derived and calculated from the trajectory data. The driver's PRT can be determined by the time interval between the onset of yellow indication and the instant in which the brake light of the target vehicle is illuminated. Considering that all recorded stopped vehicles are the first-to-stop vehicles in the lane and stop at the stop line, the deceleration rate is therefore calculated with the following equation:

$$a_{Stop} = \frac{V_0^2}{2\left(X_0 - V_0 \cdot \delta_{Stop}\right)} \tag{3}$$

where

a_{Stop} = deceleration rate (ft/s^2),
V_0 = yellow-onset speed (ft/s),
X_0 = yellow-onset distance from stop line (ft), and
δ_{Stop} = driver's PRT for stopping (s).

Second, the observed yellow-onset trajectories of all qualified first-to-stop vehicles at the four study sites are plotted on four coordinate systems, respectively, as illustrated by Figures 1*a*, 1*b*, 1*c*, and 1*d*. The vertical axis represents the vehicles' speed at the onset of yellow; the horizontal axis represents the vehicles' distance from the stop line at the onset of yellow.

Third, vehicles that have the shortest stopping distance at different speeds are identified at all four study sites, which are the circled first-to-stop vehicles shown in Figures 1*a*, 1*b*, 1*c*, and 1*d*. These identified vehicles constitute the sample for the analysis. The selection of these vehicles is in accordance with the definition of X_c, which is the minimum stopping distance that a stopped vehicle could achieve at a specific speed. Therefore, the PRT and deceleration rate of the selected samples reflect the minimum PRT ($\hat{\delta}_{Stop}$) and maximum deceleration rates ($\hat{a}_{Stop}$), respectively.

Minimum PRT Versus Speed and Other Factors

Linear regression analyses and statistical tests are conducted to test whether speed, duration of yellow time, and 85th percentile speed are significant factors influencing the driver's minimum PRT. The samples involved in the analysis are all the identified closest stopped vehicles as circled in Figures 1*a*, 1*b*, 1*c*, and 1*d*. Table 2 shows a summary of the results of the statistical analysis.

The two linear regression analyses in Table 2 aim to test whether the 85th percentile speed or duration of yellow time has a significant effect on the minimum PRT. The dependent variable for both analyses is minimum PRT. The independent variables for Analysis 1 are yellow-onset speed and 85th percentile speed; the independent variables for Analysis 2 are yellow-onset speed and duration of yellow time. *T*-tests are performed to test the significance level (*p*-value) of the independent variables in both analyses. The results summarized in Table 2 indicate that for both models, yellow-onset speed is a significant factor affecting the minimum driver's PRT at the significance level of .007, or confidence level of 99.3%. And the negative slope indicates that the higher the speed is, the shorter the minimum PRT will be. However, the *p*-values for the 85th percentile speed and the duration of yellow time are .369 and .349, respectively. Those values indicate that the 85th percentile speed and the duration of yellow time are not statistically significant factors that influence the driver's minimum PRT.

Therefore, it can be concluded that the yellow-onset speed is the only significant factor that affects the driver's minimum PRT in this study scope. A model fit test is then performed to determine the best-fit model describing the minimum PRT. The samples involved in the model fit test include all identified closest stopped vehicles. Table 3 shows a summary of the result of the test.

In Table 3 each candidate regression model has an R^2 and a *p*-value obtained from the *F* test. A higher R^2 implies that the minimum PRT is better explained by the regression model; a lower *p*-value implies a more significant effect on the minimum PRT by the yellow-onset speed. Among all candidate models, the inverse regression model has the relatively highest R^2 of .113 and the lowest *p*-value of .006. Those values reveal that the inverse model is the best-fit model that describes the relationship between the minimum PRT and the yellow-onset speed. Although the R^2 is very low, the yellow-onset speed is significant at the 99.4% confidence level. Therefore, on the basis of the result of the inverse regression summarized in Table 3, minimum PRT ($\hat{\delta}_{Stop}$) can then be modeled by a function of yellow onset speed (V_0), which is presented by the following equation:

$$\hat{\delta}_{Stop}\left(V_0\right) = 0.445 + \frac{21.478}{V_0} \tag{4}$$

Maximum Deceleration Rate Versus Speed and Other Factors

First, linear regression analyses are performed to preliminarily look at the relationship between the maximum deceleration rate

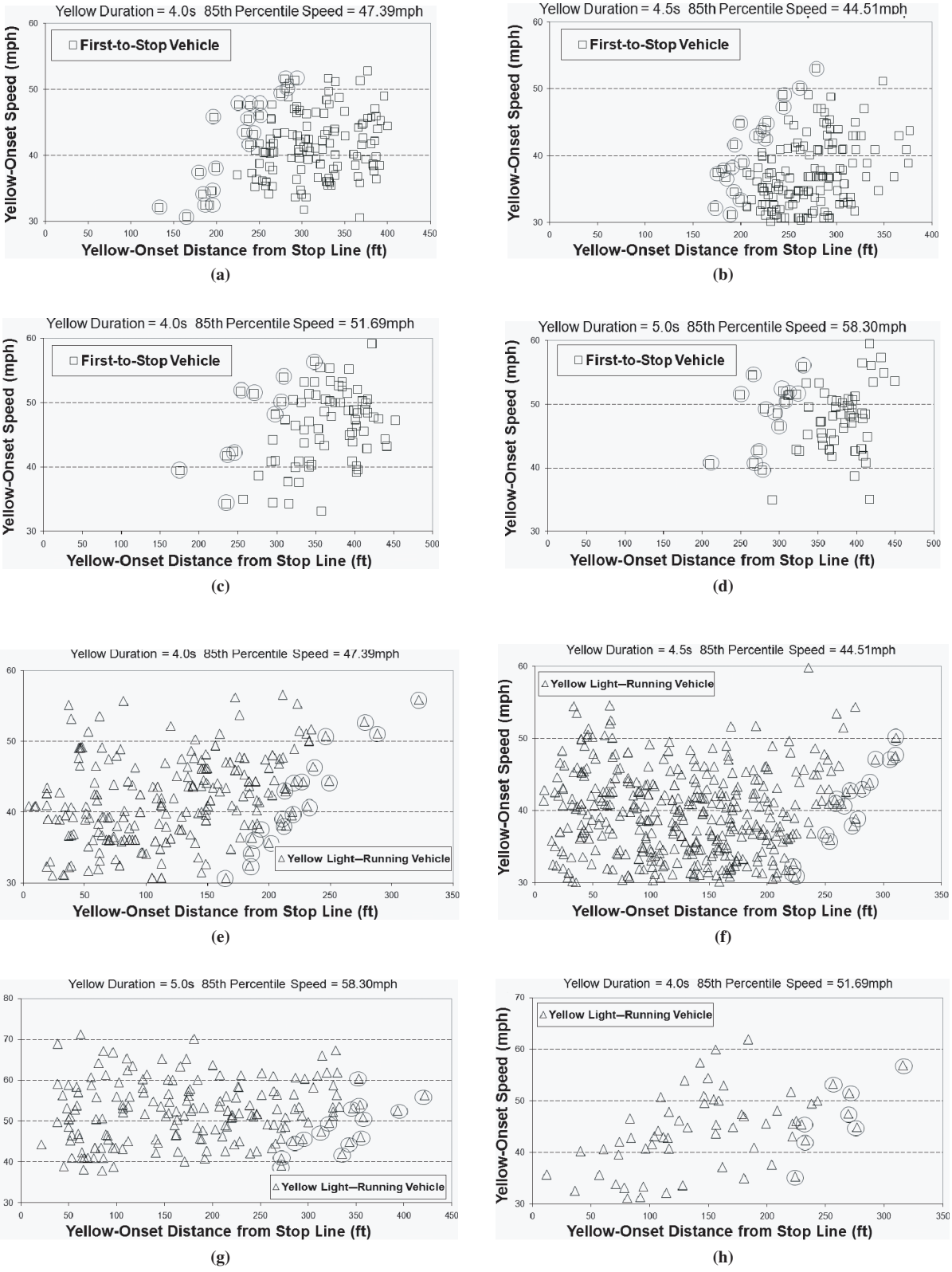

FIGURE 1 First-to-stop and yellow light running vehicles and identified samples for analysis: (*a*) first-to-stop vehicles at eastbound OH-4 at Boymel, (*b*) first-to-stop vehicles at eastbound OH-4 at Seward, (*c*) first-to-stop vehicles at westbound OH-14 at OH-44, (*d*) first-to-stop vehicles at eastbound US-50 at OH-128, (*e*) yellow light running vehicles at eastbound OH-4 at Boymel, (*f*) yellow light running vehicles at eastbound OH-4 at Seward, (*g*) yellow light running vehicles at eastbound US-50 at OH-128, and (*h*) yellow light running vehicles at westbound OH-14 at OH-44.

TABLE 2 Statistical Test Results for Potential Variables Affecting Different DZ Contributing Factors

Linear Regression Analysis	*B*	SE	*t*-Statistic	*p*-Value
Potential Variables Impacting Minimum PRT[a]				
Analysis 1				
Constant	1.246	.302	4.122	.000
Yellow-onset speed (mph)	–.013	.005	–2.797	.007
85th percentile speed (mph)	.006	.006	.905	.369
Analysis 2				
Constant	1.174	.356	3.303	.002
Yellow-onset speed (mph)	–.012	.004	–2.798	.007
Duration of yellow time (s)	.073	.077	.944	.349
Potential Variables Impacting Maximum Deceleration Rate[b]				
Analysis 1				
Constant	8.997	1.400	6.425	.000
Yellow-onset speed (mph)	.249	.022	11.262	.000
85th percentile speed (mph)	–.165	.030	–5.535	.000
Analysis 2				
Constant	5.617	1.972	2.849	.006
Yellow-onset speed (mph)	.206	.025	8.378	.000
Duration of yellow time (s)	–.663	.427	–1.552	.126
Potential Variables Impacting Maximum Acceleration Rate[c]				
Analysis 1				
Constant	7.769	1.771	4.388	.000
Yellow-onset speed (mph)	–.418	.030	–13.889	.000
85th percentile speed (mph)	.275	.039	7.036	.000
Analysis 2				
Constant	9.117	2.474	3.686	.000
Yellow-onset speed (mph)	–.352	.033	–10.653	.000
Duration of yellow time (s)	2.164	.552	3.924	.000

NOTE: SE = standard error.
[a]Dependent variable = minimum PRT; $N = 66$.
[b]Dependent variable = maximum deceleration rate; $N = 66$.
[c]Dependent variable = maximum acceleration rate; $N = 64$.

and the yellow-onset speed. Figure 2 shows results of the regression analysis.

According to Figures 2*a*, 2*b*, 2*c*, and 2*d*, all linear models have a moderate to high R^2 and a positive slope, which means the maximum deceleration rate increases as speed increases.

The comparison of the linear regression models representing different study sites is shown in Figure 2*e*. The four regression lines are sequenced down to up in a decreasing order for 85th percentile speed, revealing that under the same speed condition, the higher the 85th percentile speed of the approach is, the smaller the maximum deceleration rate will be. This finding should be a result of drivers' tendency to be more conservative at lower speed intersections than at higher speed intersections. As for the duration of yellow time, it does not seem to be a significant factor affecting the maximum deceleration rate. The reason is that the four regression lines are sequenced down to up in neither a decreasing order nor an increasing order of the duration of yellow time. These findings are supported by results of the statistical tests summarized in Table 2.

The purpose of the two analyses in the deceleration rate section of Table 2 are to test whether the 85th percentile speed or the duration of yellow time has a significant effect on the maximum deceleration rate. Results indicate that for both analyses, yellow-onset speed is a significant factor affecting the maximum deceleration rate at the significance level of .000, or confidence level of 99.9%. The *p*-value for the 85th percentile speed is also .000, which indicates that the 85th percentile speed is a statistically significant factor affecting the maximum deceleration rate at the confidence level of 99.9%. And the negative coefficient of the 85th percentile speed has proved that the maximum deceleration rate decreases as the 85th percentile speed increases. However, the *p*-value for the duration of yellow time is .126, which is higher than .05. It reveals that the duration of yellow time is not statistically significant enough to affect the maximum deceleration rate.

Therefore, it can be concluded that the yellow-onset speed and the 85th percentile speed are two significant factors affecting the maximum deceleration rate. Model fit analyses are then conducted to identify the best-fit model that describes the maximum deceleration rate. Two steps are followed to determine the best-fit relationship between each of the two independent variables (i.e., yellow-onset speed and 85th percentile speed) and the maximum deceleration rate.

First, a set of model fit tests is performed with the maximum deceleration rate as the dependent variable and the yellow-onset speed as the independent variable. For each study site, there is a particular model fit test. Samples involved in each model fit test include all the identified most closely stopped vehicles at this particular study site. Table 4 shows a summary of the results of the model fit tests.

In Table 4, each candidate regression model has an R^2, an *F* value, and a *p*-value obtained from the *F* test. A higher R^2 implies that the maximum deceleration rate is better explained by the regression model, whereas a higher *F* value implies a more significant effect on the maximum deceleration rate by the yellow-onset speed. It can be identified that the S regression model has the highest R^2 value and the highest *F* value at three of the four study sites. It is revealed that the S model best describes the relationship between the maximum

TABLE 3 Best Model Fit Analyses for Different DZ Contributing Factors: Analysis of Best-Fit Relationship Between Minimum PRT and Speed

Candidate Regression Model[a]	Model Summary				Parameter Estimate	
	R^2	*F*	Sample Size	*p*-Value	Constant	Coefficient
Linear	.100	7.109	66	.010	1.456	–.012
Logarithmic	.107	7.654	66	.007	2.854	–.506
Inverse	.113	8.144	66	.006	.445	21.478
Power	.078	5.445	66	.023	6.718	–.531
S	.081	5.640	66	.021	–.618	22.294
Exponential	.075	5.191	66	.026	1.557	–.012

[a]Dependent variable = minimum PRT; independent variable = yellow-onset speed.

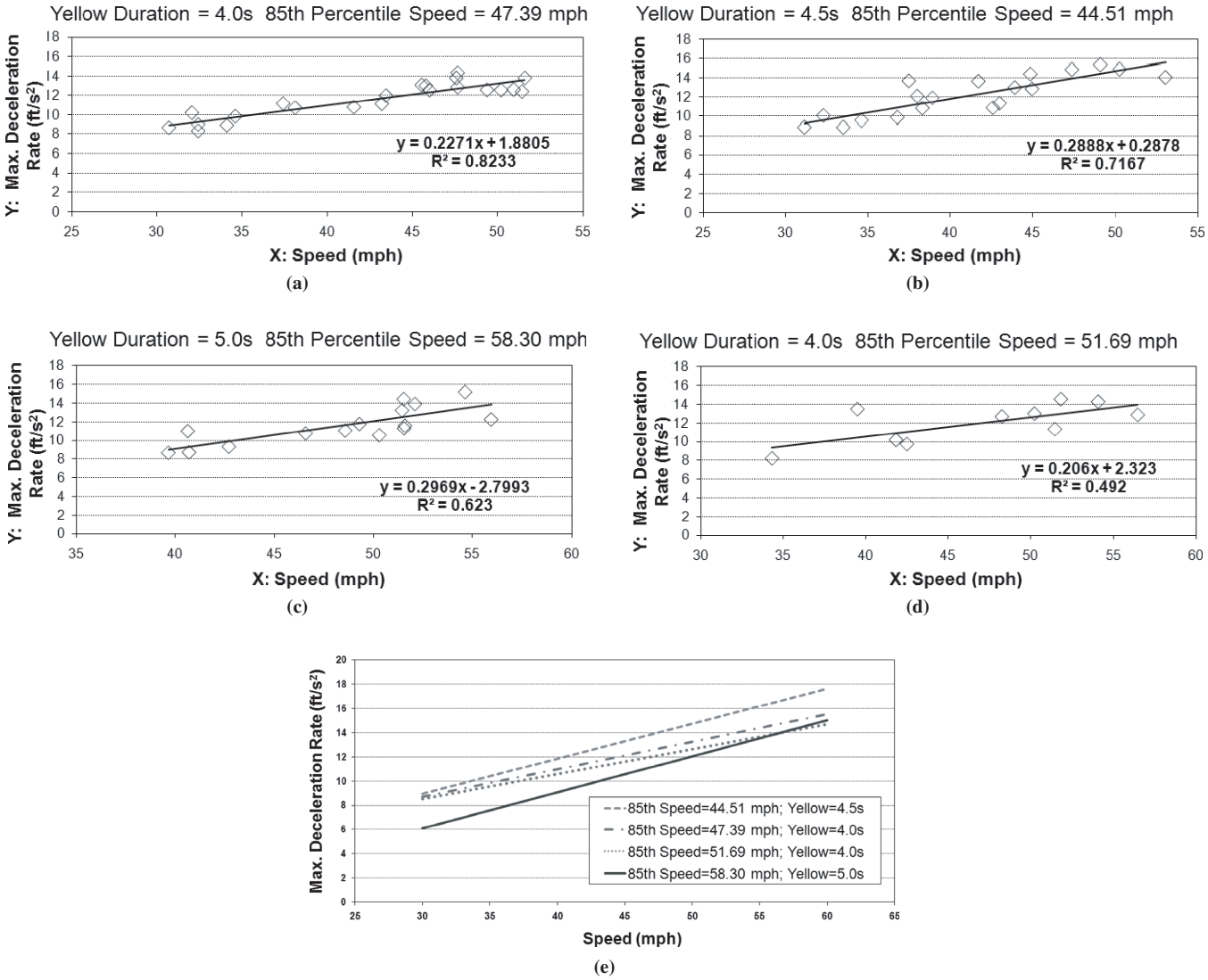

FIGURE 2 Preliminary linear regression analyses testing relation between $\hat{a}_{Stop}$ and V_0: (*a*) maximum (max.) deceleration rate versus speed eastbound OH-4 at Boymel, (*b*) maximum deceleration rate versus speed eastbound OH-4 at Seward, (*c*) maximum deceleration rate versus speed eastbound US-50 at OH-128, (*d*) maximum deceleration rate versus speed westbound OH-14 at OH-44, and (*e*) maximum deceleration rate versus speed.

deceleration rate ($\hat{a}_{Stop}$) and the yellow-onset speed (V_0). Therefore, this relationship can be represented in the following form:

$$\hat{a}_{Stop} \sim \exp\left(b_0 + \frac{b_1}{V_0}\right) \quad (5)$$

where b_0 and b_1 are the coefficients.

Second, a similar model fit analysis is performed to identify the best-fit relationship between the maximum deceleration rate ($\hat{a}_{Stop}$) and the 85th percentile speed (V_{85th}). The result finds that the inverse model represents the best-fit relationship. Therefore, this relationship can be expressed in the following form:

$$\hat{a}_{Stop} \sim b_2 + \frac{b_3}{V_{85th}} \quad (6)$$

where b_2 and b_3 are coefficients.

Finally, the best-fit regression model takes into account the relationships described by Equations 5 and 6. With the two relationships combined, the maximum deceleration rate ($\hat{a}_{Stop}$) can be modeled by a function of the yellow-onset speed (V_0) and the 85th percentile speed (V_{85th}), which is expressed by the following equation:

$$\hat{a}_{Stop}(V_0, V_{85th}) = \exp\left(b_0 + \frac{b_1}{V_0}\right) + b_2 + \frac{b_3}{V_{85th}} \quad (7)$$

where b_0, b_1, b_2, and b_3 are coefficients.

With a nonlinear regression analysis on the sample data that include all the identified most closely stopped vehicles at the four study sites, the coefficients in Equation 7 can be determined. Therefore, the final regression model of the maximum deceleration rate is represented by the following equation with an R^2 of .682:

TABLE 4 Best Model Fit Analyses for Different DZ Contributing Factors

Study Site	Candidate Regression Models	Model Summary				Parameter Estimates	
		R^2	F	Sample Size	p-Value	Constant	Coefficient
Analysis of Best-Fit Relationship Between Maximum Acceleration Rate Versus Speed[a, b]							
OH-4 at Boymel	Linear	.715	52.606	23	.000	22.366	–.456
	Logarithmic	.745	61.491	23	.000	76.585	–19.692
	Inverse	.765[d]	68.345[d]	23	.000	–16.782	820.671
OH-14 at OH-44	Linear	.802	24.306	8	.003	19.564	–.373
	Logarithmic	.835	30.413	8	.001	68.437	–17.287
	Inverse	.858[d]	36.335[d]	8	.001	–14.852	778.675
EB OH-4 at Seward	Linear	.805[d]	61.734[d]	17	.000	19.232	–.396
	Logarithmic	.798	59.251	17	.000	60.607	–15.555
	Inverse	.784	54.482	17	.000	–11.851	596.754
US-50 at OH-128	Linear	.820	63.661	16	.000	22.541	–.390
	Logarithmic	.826	66.251	16	.000	77.405	–19.044
	Inverse	.826[d]	66.305[d]	16	.000	–15.468	913.005
Analysis of Best-Fit Relationship Between Maximum Deceleration Rate Versus Speed[b, c]							
OH-4 at Boymel	Linear	.823	93.182	22	.000	1.880	.227
	Logarithmic	.835	101.468	22	.000	–23.119	9.277
	Inverse	.840	104.782	22	.000	20.502	–370.017
	Power	.844	108.137	22	.000	.478	.849
	S	.852[d]	115.216[d]	22	.000	3.256	–33.941
	Exponential	.828	96.397	22	.000	4.718	.021
OH-14 at OH-44	Linear	.492	7.749	10	.024	2.323	.206
	Logarithmic	.505	8.164	10	.021	–23.929	9.360
	Inverse	.514	8.470	10	.020	21.042	–415.250
	Power	.538	9.332	10	.016	.431	.863
	S	.553[d]	9.893[d]	10	.014	3.307	–38.437
	Exponential	.520	8.675	10	.019	4.862	.019
EB OH-4 at Seward	Linear	.717	43.016	19	.000	.288	.289
	Logarithmic	.728	45.575	19	.000	–31.969	11.910
	Inverse	.731	46.110	19	.000	24.044	–477.851
	Power	.734	46.816	19	.000	.283	1.010
	S	.742[d]	48.980[d]	19	.000	3.496	–40.718
	Exponential	.716	42.807	19	.000	4.393	.024
US-50 at OH-128	Linear	.623	21.482	15	.000	–2.799	.297
	Logarithmic	.618	21.040	15	.001	–42.027	13.837
	Inverse	.611	20.396	15	.001	24.910	–637.913
	Power	.659	25.069	15	.000	.095	1.236
	S	.654	24.539	15	.000	3.629	–57.103
	Exponential	.661[d]	25.305[d]	15	.000	3.173	.026

[a]Dependent variable = maximum acceleration rate.
[b]Independent variable = yellow-onset speed.
[c]Dependent variable = maximum deceleration rate.
[d]Indicates the highest R^2 or F value in the group.

$$\hat{a}_{\text{Stop}}(V_0, V_{85\text{th}}) = \exp\left(3.379 + \frac{-36.099}{V_0}\right) - 9.722 + \frac{429.692}{V_{85\text{th}}} \quad (8)$$

ANALYSIS OF MAXIMUM ACCELERATION RATE

Preparation of Data Samples

First, the PRT for running and the acceleration rate of each yellow light running vehicle needs to be obtained. PRT for running is difficult to measure accurately with the video-capture-based techniques applied in this study. However, on the basis of the assumption that drivers use the same PRT for making a go decision compared with making a stop decision in response to the yellow indication, in this paper the PRT for running is considered the same as the PRT for stopping. As for the acceleration rate, it can be derived and calculated from the trajectory data. The following equation represents that calculation:

$$a_{\text{Run}} = \frac{2(X_0 - V_0 \cdot t)}{(t - \delta_{\text{Run}})^2} \quad (9)$$

where

a_{Run} = acceleration rate (ft/s^2),
t = time interval between the onset of yellow and the instant when the vehicle passes the stop line (s), and
δ_{Run} = driver's PRT for running (s).

Second, the observed yellow-onset trajectories of all qualified yellow light running vehicles at the four study sites are plotted on the four coordinate systems, as illustrated by Figures 1*e*, 1*f*, 1*g*, and 1*h*. The vertical axis represents vehicle speed at the onset of yellow, and the horizontal axis represents vehicle yellow-onset distance from stop line.

Third, vehicles that have the farthest running distance at different speeds are identified at the four study sites; they are the circled yellow light running vehicles shown in Figures 1*e*, 1*f*, 1*g*, and 1*h*. These identified vehicles constitute the sample for the analysis. The selection of these vehicles is in accordance with the definition of X_0, which is the maximum yellow light running distance that a vehicle could make at a specific speed. Therefore, the acceleration rate of each selected sample reflects the maximum acceleration rate ($\hat{a}_{\text{Run}}$). When $\hat{a}_{\text{Run}}$ is derived for each selected sample, $\hat{\delta}_{\text{Stop}}$ is used instead in the calculation of $\hat{a}_{\text{Run}}$ because $\hat{\delta}_{\text{Run}}$ is assumed to be equal to $\hat{\delta}_{\text{Stop}}$.

$$\hat{\delta}_{\text{Run}}(V_0) = \hat{\delta}_{\text{Stop}}(V_0) = 0.445 + \frac{21.478}{V_0} \tag{10}$$

Maximum Acceleration Rate Versus Speed and Other Factors

Similar to the analysis of the maximum deceleration rate, linear regression analysis is used preliminarily to test how the yellow-onset speed and the maximum acceleration rate are potentially related. Figure 3 shows the results of this regression analysis.

According to Figures 3*a*, 3*b*, 3*c*, and 3*d*, all the linear models have moderate to high R^2 values and a negative slope, which means the maximum acceleration rate tends to decrease as speed increases. The reason is that drivers do not need to use a high acceleration rate to pass through the intersection when they are traveling at a high speed. Some maximum acceleration rates are negative in Figures 3*a*, 3*b*, 3*c*, and 3*d* in instances in which the traveling speed of the vehicle is higher than the 85th percentile speed. It reveals that when drivers are going through the intersection at a relatively high speed, they will probably release the gas pedal, or slightly apply the brake through cautiousness.

Figure 3*e* shows a comparison of the linear regression models representing the relationship between the maximum acceleration

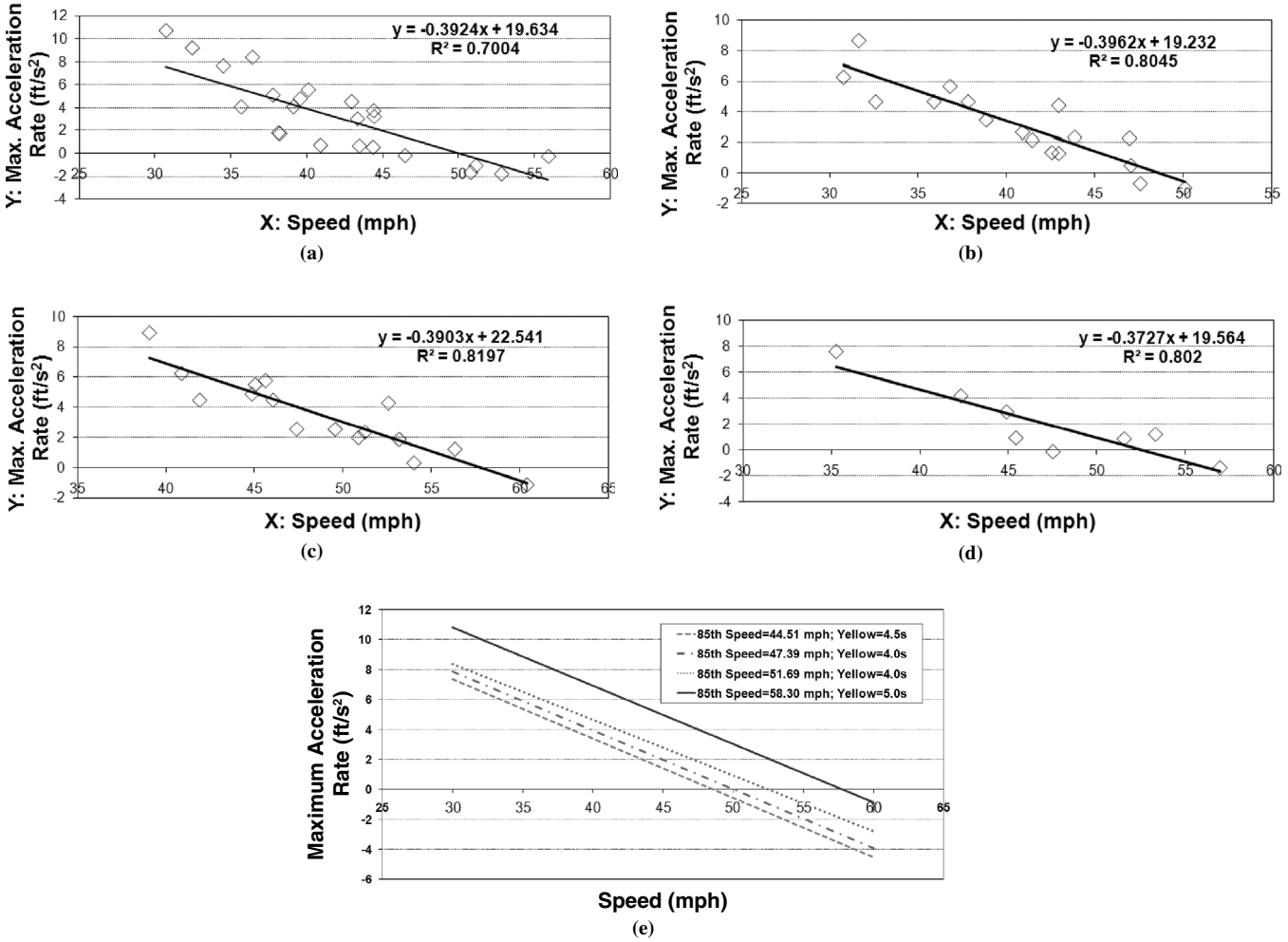

FIGURE 3 Preliminary linear regression analyses testing relation between $\hat{a}_{\text{Run}}$ and V_0: (*a*) maximum acceleration rate versus speed at eastbound OH-4 at Boymel (yellow duration = 4.0 s; 85th percentile speed = 47.39 mph), (*b*) maximum acceleration rate versus speed at eastbound OH-4 at Seward (yellow duration = 4.5 s; 85th percentile speed = 44.51 mph), (*c*) maximum acceleration rate versus speed at eastbound US-50 at OH-128 (yellow duration = 5.0 s; 85th percentile speed = 58.30 mph), (*d*) maximum acceleration rate versus speed at eastbound OH-14 at OH-44 (yellow duration = 4.0 s; 85th percentile speed 51.69 mph), and (*e*) maximum acceleration rate versus speed.

rate and speed for the four study sites. The four regression lines are sequenced down to up in an increasing order of the 85th percentile speed. This result means that under the same speed condition, the higher the 85th percentile speed of the intersection approach is, the greater the maximum acceleration rate will be. This finding should be the result of drivers' tendency to be more aggressive at higher speed intersections than at lower speed intersections. As for the duration of yellow time, the four regression lines are sequenced down to up in neither a decreasing order nor an increasing order of the duration of yellow time. These findings are supported by results of the statistical tests summarized in Table 2.

The two analyses in the acceleration rate section of Table 2 are done to test whether the 85th percentile speed or the duration of yellow time has a significant effect on the maximum acceleration rate. Results indicate that for both models, yellow-onset speed is a significant factor affecting the maximum acceleration rate at the significance level of .000, or confidence level of 99.9%. The *p*-value for the 85th percentile speed is .000, which indicates that the 85th percentile speed is a statistically significant fact that affects the maximum acceleration rate at the confidence level of 99.9%. And its positive coefficient has proved that the maximum acceleration rate increases as the 85th percentile speed increases. As for the duration of yellow time, the *p*-value is also .000, and the slope is positive. Statistically the meaning is that the duration of yellow time also has a significant effect on the maximum acceleration rate. And the positive slope means that the longer the yellow time is, the larger the maximum acceleration rate will be. However, the positive slope is contributed mainly by the big difference in the maximum acceleration rate between 5.0-s yellow time and 4.0-s/4.5-s yellow time. According to Figure 3*e*, the regression line representing the 4.5-s yellow time is located even lower than the regression lines representing the yellow time of 4.0 s. This result is a conflict with the positive slope.

Therefore, it can be concluded that in addition to the yellow-onset speed, only the 85th percentile speed is an actually significant factor affecting the maximum acceleration rate. To determine the best-fit model of the maximum acceleration rate, two steps are needed because there are two independent variables (i.e., speed and 85th percentile speed).

First, a set of model fit tests is performed with the maximum acceleration rate as the dependent variable and the yellow-onset speed as the independent variable. Samples involved in each model fit test include all identified vehicles with the farthest running distances at this particular study site. Results of the model fit tests are summarized in Table 4.

In Table 4, there are only three candidate regression models because only these three models can have negative dependent variable values. The inverse model is shown to be the best-fit model that best describes the relationship between the maximum acceleration rate ($\hat{a}_{\text{Run}}$) and the yellow-onset speed (V_0) because it has the highest R^2 value and the highest F value at three of the four study sites. Therefore, the relationship can be represented in the following form:

$$\hat{a}_{\text{Run}} \sim b_0 + \frac{b_1}{V_0} \tag{11}$$

where b_0 and b_1 are coefficients.

Second, similar model fit analysis is performed to identify the best-fit relationship between the maximum acceleration rate ($\hat{a}_{\text{Run}}$) and the 85th percentile speed ($V_{85\text{th}}$). The result identifies the linear model to be the best-fit model. Therefore, the relationship can be represented in the following form:

$$\hat{a}_{\text{Run}} \sim b_2 \cdot V_{85\text{th}} + b_3 \tag{12}$$

where b_2 and b_3 are the coefficients.

Finally, the best-fit regression model takes into account both relationships described by Equations 11 and 12. By combining the two relationships, the final regression model is a function of the yellow-onset speed (V_0) and the 85th percentile speed ($V_{85\text{th}}$), which is expressed by the following equation:

$$\hat{a}_{\text{Run}}\left(V_0, V_{85\text{th}}\right) = b_0 + \frac{b_1}{V_0} + b_2 \cdot V_{85\text{th}} \tag{13}$$

where b_0, b_1, and b_2 are coefficients.

By performing a nonlinear regression analysis on the sample data that include all identified vehicles with the farther running distances at the four study sites, the coefficients in Equation 13 are determined. Therefore, the final regression model of the maximum acceleration rate is represented by the following equation with an R^2 value of .775:

$$\hat{a}_{\text{Run}}\left(V_0, V_{85\text{th}}\right) = -27.91 + \frac{760.258}{V_0} + 0.266 \cdot V_{85\text{th}} \tag{14}$$

CONCLUSIONS

Results of the statistical analyses conducted on the yellow phase trajectory data have proved the dynamic features of the contributing factors for Type I DZ and option zone. The highlights of the results are summarized as follows:

- The minimum PRT is significantly affected by speed. Mathematically, PRT is a function of speed described by the inverse model. The minimum PRT decreases as the speed increases.
- The maximum deceleration rate is significantly affected by speed and the 85th percentile speed of the intersection approach. Mathematically, the maximum deceleration rate is described by the summation of an S model of speed and an inverse model of the 85th percentile speed. The maximum deceleration rate increases as the speed increases. And under the same speed condition, the higher the 85th percentile speed of the intersection approach, the smaller the maximum deceleration rate will be.
- The maximum acceleration rate is also significantly affected by both speed and 85th percentile speed of the intersection approach. Mathematically, the rate is represented by the summation of an inverse model of speed and a linear model of the 85th percentile speed. The maximum acceleration rate decreases as the speed increases. And under the same speed condition, the higher the 85th percentile speed of the intersection approach, the larger the maximum acceleration rate will be.

On the basis of these new findings, the final modified GHM model for dynamic DZ is determined by removing the insignificant

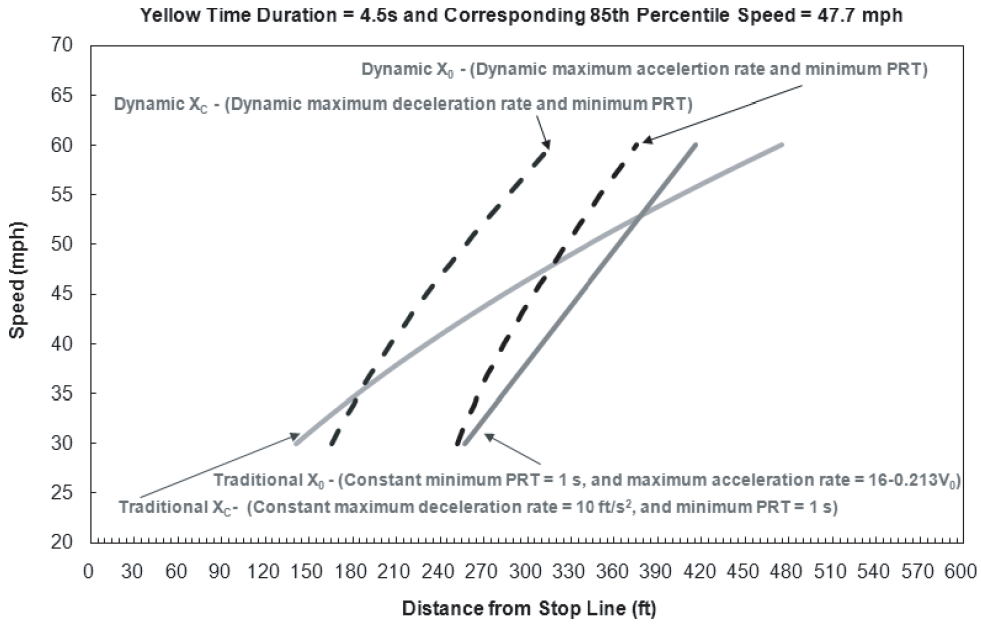

FIGURE 4 Comparison between traditional and dynamic DZs.

factors from Equations 1 and 2 and is represented by the following equations:

$$X_c(V_0, V_{85th}) = V_0\hat{\delta}_{Stop}(V_0) + \frac{V_0^2}{2 \cdot \hat{a}_{Stop}(V_0, V_{85th})} \quad (15)$$

$$X_0(V_0, \tau, V_{85th}) = V_0\tau + \frac{1}{2}\hat{a}_{Run}(V_0, V_{85th}) \cdot [\tau - \delta_{Run}(V_0)]^2 \quad (16)$$

With incorporation of the regression equations of $\hat{a}_{Stop}$, $\hat{a}_{Run}$, $\hat{\delta}_{Stop}$, and $\hat{\delta}_{Run}$, Equations 15 and 16 are therefore updated as follows:

$$X_c(V_0, V_{85th}) = V_0\left(0.445 + \frac{21.478}{V_0}\right) + \frac{V_0^2}{2 \cdot \left[\exp\left(3.379 + \frac{-36.099}{V_0}\right) - 9.722 + \frac{429.692}{V_{85th}}\right]} \quad (17)$$

$$X_0(V_0, \tau, V_{85th}) = V_0\tau + \frac{1}{2}\left(-27.91 + \frac{760.258}{V_0} + 0.266 \cdot V_{85th}\right) \cdot \left[\tau - \left(0.445 + \frac{21.478}{V_0}\right)\right]^2 \quad (18)$$

One significant application or implementation of the calibrated dynamic DZ model is updating the DZ table, which was originally established on the basis of the traditional DZ model. Typically, the traditional DZ table assumes constant minimum PRT and maximum deceleration of 1 s and 10 ft/s^2, respectively, suggested by ITE. The maximum acceleration rate is assumed to be computed with the following equation:

$$\hat{a}_{Run} = 16.0 - 0.213 \times V_0 \quad (19)$$

Figure 4 shows the comparison between the traditional and dynamic DZs with a 4.5-s yellow time setting and the corresponding 47.7-mph 85th percentile speed as an example. At higher speeds, the traditional X_c tends to be much farther from the stop line when compared with the dynamic X_c, and the traditional X_0 tends to be much farther from the stop line when compared with the dynamic X_0. According to the lines representing the traditional X_c and X_0, the Type I DZ forms when the speed is higher than 53 mph. However, the option zone always exists from 30 mph through 60 mph according to the lines representing the dynamic X_c and X_0. The dynamic DZ model was calibrated with field-observed data, indicating that the traditional DZ model fails to describe real-world driving behavior. In essence, the reason is that it is difficult to reflect the dynamic features of the DZ with the traditional model. Therefore, the new dynamic model has proved to be capable of providing a theoretical base to update the existing DZ tables as ones that are dynamic with the identified characteristics of the contributing factors.

ACKNOWLEDGMENTS

The research presented in this paper was supported by a grant funded by the Ohio Department of Transportation and FHWA. The authors sincerely appreciate the assistance offered during the data collection phase by Qingyi Ai, Bei Zhao, and Sudhir R. Itekyala of the University of Cincinnati, as well as Ashim Garg and Chun Shao of the University of Akron.

REFERENCES

1. Gazis, D., R. Herman, and A. Maradudin. The Problem of the Amber Signal Light in Traffic Flow. *Operations Research*, Vol. 8, No. 1, 1960, pp. 112–132.
2. Pant, P. D., Y. Cheng, A. Rajagopal, and N. Kashayi. *Field Testing and Implementation of Dilemma Zone Protection and Signal Coordination at Closely Spaced High Speed Intersections.* Report FHWA/OH-2005/006. Ohio Department of Transportation, Columbus, 2005.

3. Liu, Y., G. L. Chang, R. Tao, T. Hicks, and E. Tabacek. Empirical Observations of Dynamic Dilemma Zones at Signalized Intersections. In *Transportation Research Record: Journal of the Transportation Research Board, No. 2035,* Transportation Research Board of the National Academies, Washington, D.C., 2007, pp. 122–133.
4. Tarko, A. P., W. Li, and L. Laracuente. Probabilistic Approach to Controlling Dilemma Occurrence at Signalized Intersections. In *Transportation Research Record: Journal of the Transportation Research Board, No. 1973,* Transportation Research Board of the National Academies, Washington, D.C., 2006, pp. 55–63.
5. Moon, Y., and F. Coleman III. Dynamic Dilemma Zone Based on Driver Behavior and Car-Following Model at Highway–Rail Intersections. *Transportation Research Part B,* Vol. 37, No. 4, 2002, pp. 323–344.
6. Kim, W., J. Zhang, A. Fujiwara, T. Y. Jang, and N. Moon. Analysis of Stopping Behavior at Urban Signalized Intersections: Empirical Study in South Korea. In *Transportation Research Record: Journal of the Transportation Research Board, No. 2080,* Transportation Research Board of the National Academies, Washington, D.C., 2008, pp. 84–91.
7. Zegeer, C. *Effectiveness of Green-Extension Systems at High-Speed Intersections.* Research Report 472. Kentucky Department of Transportation, Frankfort, 1977.
8. Elmitiny, N., X. Yan, E. Radwan, C. Russo, and D. Nashar. Classification Analysis of Driver's Stop/Go Decision and Red Light Running Violation. *Accident Analysis and Prevention,* Vol. 42, No. 1, 2010, pp. 101–111.
9. Sharma, A., D. M. Bullock, and S. Peeta. Limitations of Simultaneous Gap-Out Logic. In *Transportation Research Record: Journal of the Transportation Research Board, No. 1978,* Transportation Research Board of the National Academies, Washington, D.C., 2006, pp. 42–48.
10. Sharma A., D. M. Bullock, and S. Peeta. Recasting Dilemma Zone Design as a Marginal Cost–Benefit Problem. In *Transportation Research Record: Journal of the Transportation Research Board, No. 2035,* Transportation Research Board of the National Academies, Washington, D.C., 2007, pp. 88–96.
11. Parsonson, P. S. *NCHRP Synthesis of Highway Practice 172: Signal Timing Improvement Practices.* TRB, National Research Council, Washington, D.C., 1992.
12. Zimmerman, K., J. A. Bonneson, D. Middleton, and M. M. Abbas. Improved Detection and Control System for Isolated High-Speed Signalized Intersections. In *Transportation Research Record: Journal of the Transportation Research Board, No. 1856*, Transportation Research Board of the National Academies, Washington, D.C., 2003, pp. 212–219.
13. Zimmerman, K., and J. A. Bonneson. Intersection Safety at High-Speed Signalized Intersections: Number of Vehicles in Dilemma Zone as Potential Measure. In *Transportation Research Record: Journal of the Transportation Research Board, No. 1897,* Transportation Research Board of the National Academies, Washington, D.C., 2004, pp. 126–133.
14. Si, J., T. Urbanik II, and L. D. Han. Effectiveness of Alternative Detector Configurations for Option Zone Protection on High-Speed Approaches to Traffic Signals. In *Transportation Research Record: Journal of the Transportation Research Board, No. 2035,* Transportation Research Board of the National Academies, Washington, D.C., 2007, pp. 107–113.
15. Urbanik, T., and P. Koonce. The Dilemma with Dilemma Zones. *Proc., ITE District 6 Annual Meeting,* Portland, Ore., 2007.
16. Saito, T., N. Ooyama, and K. Sigeta. Dilemma and Option Zones, the Problem and Countermeasures-Characteristics of Zones, and a New Strategy of Signal Control for Minimizing Zones. *Proc., 3rd International Conference on Road Traffic Control,* London, Institute of Electrical Engineers, London, 1990, pp. 137–141.
17. Koll, H., M. Bader, and K. W. Axhausen. Driver's Behavior During Flashing Green Before Amber: A Comparative Study. *Accident Analysis and Prevention,* Vol. 36, No. 2, 2004, pp. 273–280.
18. Chang, G., H. Xiang, and C. Chou. *Interrelations Between Crash Rates, Signal Yellow Times, and Vehicle Performance Characteristics: Phase I.* Research Report MD-04-SP308B4L. Maryland State Highway Administration, Maryland Department of Transportation, Baltimore, 2004.
19. ITE. *Traffic Engineering Handbook.* Prentice Hall, Upper Saddle River, N.J., 1999.
20. *Traffic Detector Handbook,* 3rd ed. FHWA, U.S. Department of Transportation, 2006.
21. Click, S. M. Application of the ITE Change and Clearance Interval Formulas in North Carolina. *ITE Journal,* Vol. 78, No. 1, 2008, pp. 20–24.
22. Li, Z. Daniel B. Fambro Student Paper Award: Modeling Dynamic Dilemma Zones Using Observed Yellow-Onset Trajectories. *ITE Journal,* Vol. 79, No. 11, 2009, pp. 24–35.
23. Wei, H., Z. Li, and Q. Ai. Observation-Based Study of Intersection Dilemma Zone Natures. *Journal of Safety & Security,* Vol. 1, No. 4, 2009, pp. 282–295.
24. Wei, H., E. Meyer, J. Lee, and C. E. Feng. Video-Capture-Based Approach to Extract Multiple Vehicular Trajectory Data for Traffic Modeling. *ASCE Journal of Transportation Engineering,* Vol. 131, No. 7, 2005, pp. 496–505.

The results and ideas presented in this paper reflect the authors' points of view.

The Traffic Signal Systems Committee peer-reviewed this paper.